separations

MDPI

Supplementary Materials

Identification of Soluble Degradation Products in Lithium–Sulfur and Lithium–Metal Sulfide Batteries

Fabian Horsthemke [1], Christoph Peschel [1], Kristina Kösters [1], Sascha Nowak [1], Kentaro Kuratani [2], Tomonari Takeuchi [2], Hitoshi Mikuriya [3], Florian Schmidt [4], Hikari Sakaebe [2], Stefan Kaskel [4], Tetsuya Osaka [3,5], Martin Winter [1,6], Hiroki Nara [3,*] and Simon Wiemers-Meyer [1,*]

1 MEET Battery Research Center, University of Münster, Corrensstraße 46, 48149 Münster, Germany; f.horsthemke@uni-muenster.de (F.H.); christoph.peschel@uni-muenster.de (C.P.); kristina.koesters@uni-muenster.de (K.K.); sascha.nowak@uni-muenster.de (S.N.); martin.winter@uni-muenster.de (M.W.)
2 Research Institute of Electrochemical Energy, Department of Energy and Environment, National Institute of Advanced Industrial Science and Technology (AIST), Ikeda, Osaka 563-8577, Japan; k-kuratani@aist.go.jp (K.K.); takeuchi.tomonari@aist.go.jp (T.T.); hikari.sakaebe@aist.go.jp (H.S.)
3 Research Organization for Nano & Life Innovation, Waseda University, Tokyo 162-0041, Japan; h.mikuriya@aoni.waseda.jp (H.M.); osakatets@waseda.jp (T.O.)
4 Department of Chemistry, Technische Universität Dresden, 01062 Dresden, Germany; florian.schmidt@iws.fraunhofer.de (F.S.); stefan.kaskel@tu-dresden.de (S.K.)
5 Faculty of Science and Engineering, Waseda University, Tokyo 169-8555, Japan
6 Helmholtz Institute Münster, IEK-12, Forschungszentrum Jülich, Corrensstraße 46, 48149 Münster, Germany
* Correspondence: h-nara@aoni.waseda.jp (H.N.); simon.wiemers-meyer@uni-muenster.de (S.W.-M.)

Citation: Horsthemke, F.; Peschel, C.; Kösters, K.; Nowak, S.; Kuratani, K.; Takeuchi, T.; Mikuriya, H.; Schmidt, F.; Sakaebe, H.; Kaskel, S.; et al. Identification of Soluble Degradation Products in Lithium–Sulfur and Lithium–Metal Sulfide Batteries. *Separations* **2022**, *8*, 57. https://doi.org/10.3390/separations9030057

Academic Editor: Mark L. Dietz

Received: 17 January 2022
Accepted: 13 February 2022
Published: 24 February 2022

Publisher's Note: MDPI stays neutral with regard to jurisdictional claims in published maps and institutional affiliations.

1. Experimental

Three layered pouch cells with sulfurized poly(acrcrylonitrile) (SPAN)-based cathode active material (CAM) [26] and the following composition SPAN with vapor grown carbon nanofibers (VGCF) or Ketjen black as conductive additive (CA) and a mixture of carboxymethyl cellulose (CMC)/styrene-butadiene rubber (SBR) (2/1) was used as binder. The ratio of the components was CAM:CA:binder; 97.3:30:3 coated on aluminum foam current collectors (see Nara et. al. [2]). The cells were shipped to MEET Battery Research Center after electrochemical aging (20 cycles at around 0.45 mA cm^{-2} between 1.0 V and 3.0 V) performed by the authors from WASEDA University. The applied electrolyte was 1 mol L^{-1} LiTFSI in DOL/DME (1:1; v:v).

For all following cells with standard LiS CAM the lithium foil was roll-pressed from 500 µm to 350 µm according to Becking et al. [27] Afterwards disks of 12 mm diameter were punched and combined with Celgard2500 separators (Celgard; Charlotte, NC., USA) for the coin cell assembly.

The cathode active material consisted of sulfur melt infiltrated into Ketjen black (C/S) mixed with multi-walled carbon nanotubes (Nanocyl MWCNT) and poly(tetrafluoroethylene) (PTFE) in a weight ratio of 90:7:3 (C/S:MWCNT:PTFE) to give a sulfur content of 60 wt% in the final electrode (similar to Weller et al. [28]). Lithium-sulfur cells with 60 µL of ether-based electrolyte (0.25 mol L^{-1} $LiNO_3$ and 1 mol L^{-1} LiTFSI in DOL/DME; 1:1; w:w) or carbonate-based electrolyte (1 mol L^{-1} $LiPF_6$ in EC/DMC; 1:1; w:w) were built with 14 mm disks of standard LiS cathodes The cells were cycled at 0.66 mA cm^{-2} for the first three cycles and at 0.2 mA cm^{-2} in a voltage window of 1.8 V to 2.6 V until 100 cycles were reached.

Cathodes with titanium sulfide as active material (see Sakuda et al. [23]) were used in two-electrode coin cells with Celgard2500 separator (Celgard; Charlotte, NC., USA) and 60 µL of electrolyte (1 mol L^{-1} $LiPF_6$ in DMC/EC; 1:1; w:w). The weight ration of TiS_4, Ketjen Black (KB) and binder was 79:8:13. The cells were cycled in a voltage window of

1.9 V to 3.0 V with 0.02 mA cm^{-2} for the first thee cycles and at 0.06 mA cm^{-2} until 100 cycles were reached.

Results and Discussion

The cyclic aging of the different cells is exemplarily shown in Figures S1-4. The electrolytes were regained at the end of the respective cycling procedure and investigated using the different GC and IC setups and protocols.

Figure S1 shows the cyclic aging of an LiS cell with sulfur melt infiltrated into meso/macroporous carbon material. The voltage plot shows the plateaus which are characteristic for LiS chemistries and a good capacity retention over the applied 100 cycles was obtained.

The capacity retention and voltage profile of one exemplary cell with SPAN-based active material is displayed in Figure S2. The cell shows a stable capacity retention and a voltage profile already reported for this cell chemistry [26].

The standard LiS setup with sulfur melt infiltrated in meso/macroporous carbon and a carbonate-based electrolyte shows a strong deterioration already in the first discharge cycle (Figure S3). Moreover, the initial discharge capacity is much lower compared to the cells build with similar electrodes using ether-based electrolytes (Figure S1). This phenomenon shows that the decomposition reactions alter the electrochemical behavior of the active material already at low states-of-charge. Furthermore, the capacity retention of the cell is poor and reduced to polarization and related phenomena after the first cycle. Since this setup was built as worst-case-scenario and the carbonates directly react with the formed polysulfides this behavior was expected.

The voltage profiles of an exemplary cell with titanium-based active material and carbonate-based electrolytes are shown in Figure S4. The cell shows a stable cycling performance with a steady loss of capacity over the course of the applied 100 charge discharge cycles.

2. Figures

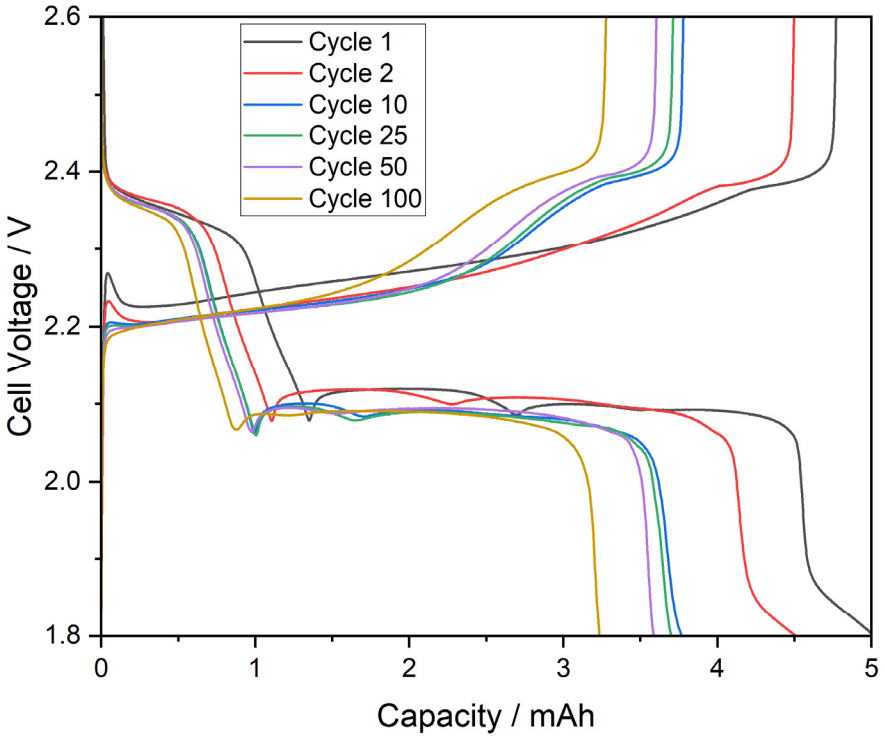

Figure S1. Cell voltage versus capacity plots of different charge/discharge cycles from a standard LiS cell with ether-based electrolyte.

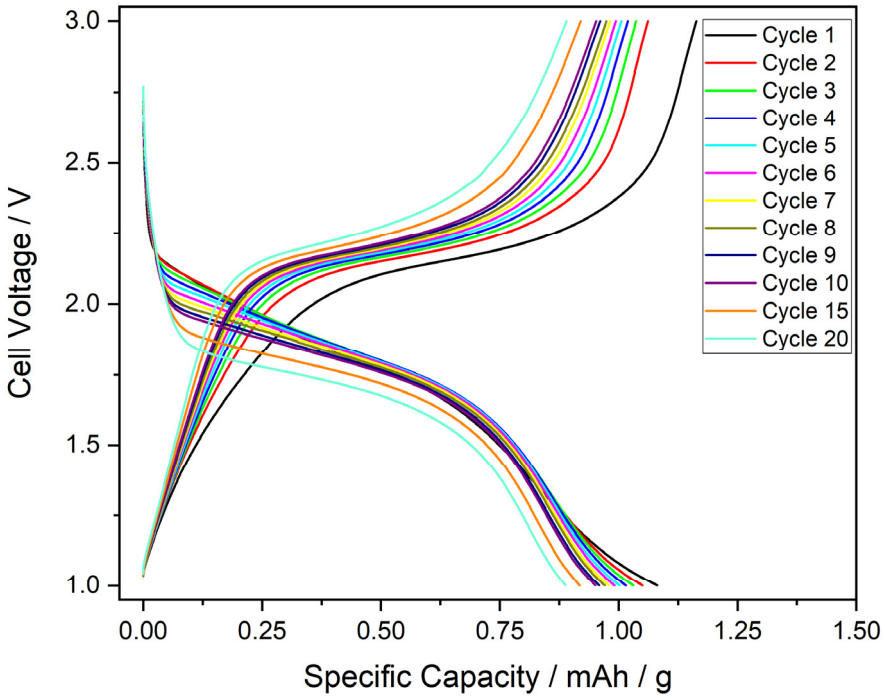

Figure S2. Cell voltage versus specific capacity (mass of sulfur) plots of different charge/discharge cycles of a cell with SPAN as active material on an aluminum foam current collector. VGCF was used as conductive additive and the electrolyte was ether-based.

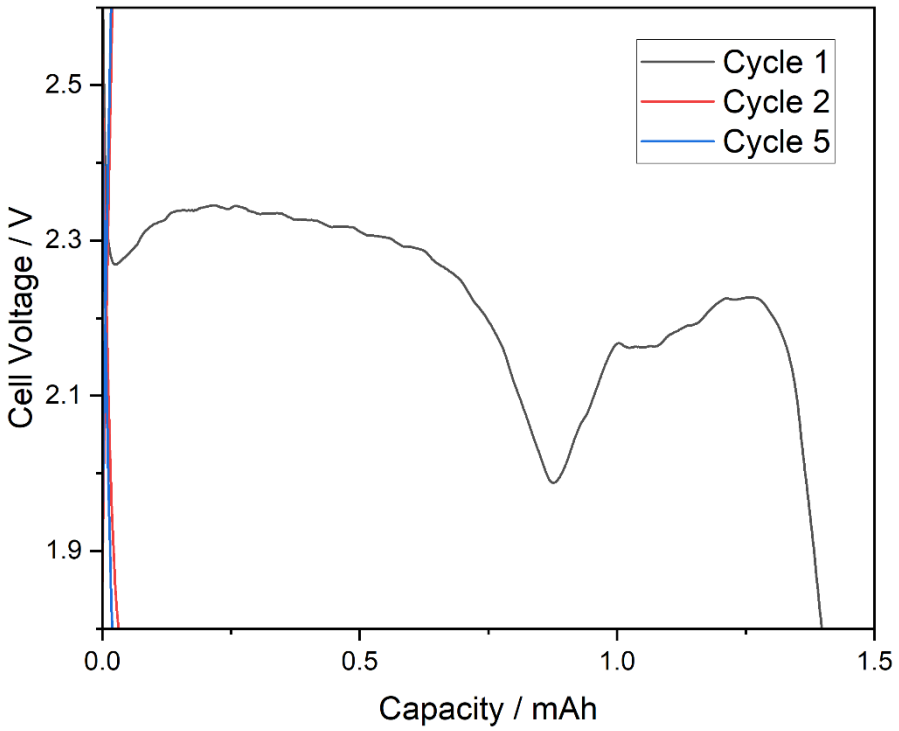

Figure S3. Cell voltage versus capacity plot of a cell built with standard LiS cathodes and carbonate-based electrolyte.

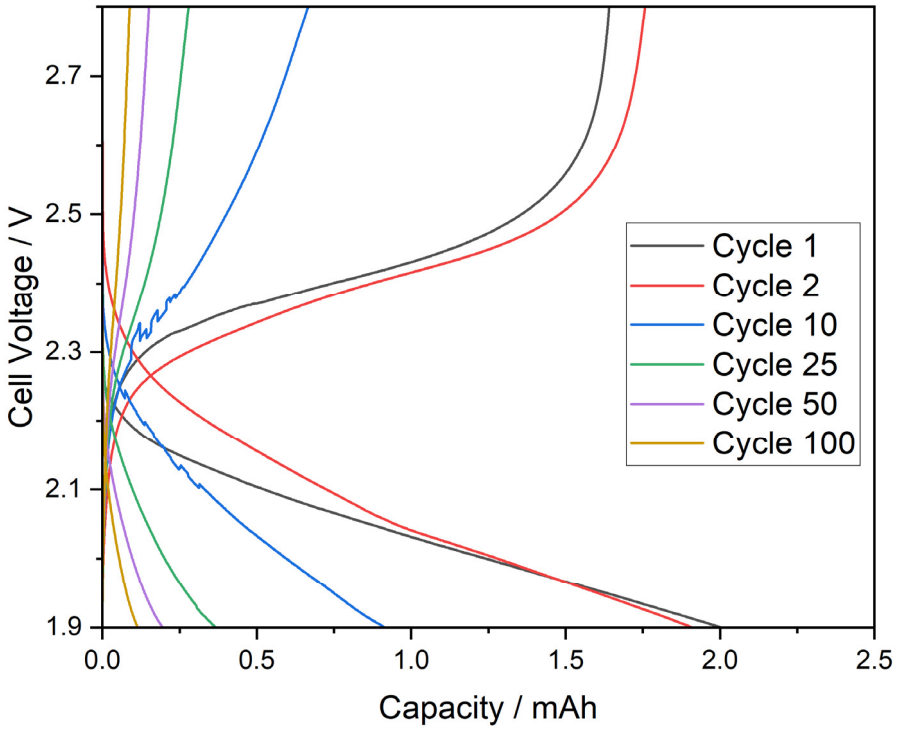

Figure S4. Cell voltage versus capacity plots of charge/discharge cycles of a cell with TiS_4 as active material and carbonate-based electrolyte. Unsteady cell voltage of cycle 10 could be caused by micro short circuits, due to dendrite growth through the rather thin Celgard2500 separator.